

**Supporting information:**  
**Bistability and oscillatory motion of natural nano-membranes appearing within  
monolayer graphene on silicon dioxide**

T. Mashoff, M. Pratzner, V. Geringer, T. J. Echtermeyer, M. C. Lemme, M. Liebmann, and M. Morgenstern

**I. DETERMINATION OF THE POSITION OF  
BUMPS IN STRESSED GRAPHENE AREAS**

Fig. 1a) shows a three dimensional representation of a graphene surface consisting of a lifted valley surrounded by stable hills (tunneling parameters:  $U = 0.4$  V,  $I = 2$  nA). Analyzing the atomically resolved STM image in detail, we find a hexagonal arrangement of the carbon atoms at the hills, as expected for monolayer graphene (see blue hexagon in Fig. 1b). In contrast, within the stressed area we observe a triangular appearance of bright bumps at every second atom. By following up the line in Fig. 1b) one clearly sees that the bumps within the stressed area do not appear in the center of the hexagons but at one of the atomic sites providing a symmetry breaking between A and B lattice. The ball model presented in Fig. 1a) illustrates a possible atomic arrangement explaining the broken symmetry induced by the compressive stress. To reduce the stress a zig-zag like arrangement of the carbon atoms is favoured.

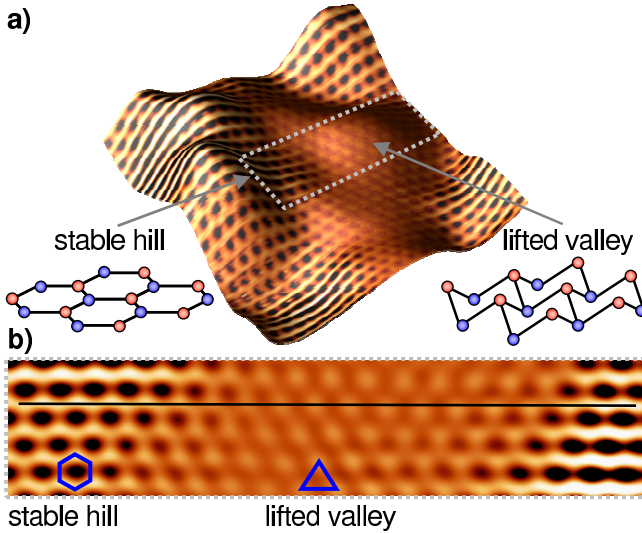


FIG. 1: a) Atomically resolved STM image of a graphene surface consisting of relaxed (hills) and a stressed area (lifted valley). The ball model explains the broken symmetry between A (blue balls) and B (orange balls) lattice of graphene due to compressive stress. b) Magnification of the dotted area marked in a). The changing atomic arrangement from relaxed (hexagons) to stressed (triangles) graphene areas can be identified.

**II. DETERMINATION OF THE INITIAL  
TIP/GRAPHENE DISTANCE  $z_{tg}^0$  AND THE  
DECAY CONSTANT  $\kappa(U)$**

The absolute distance between tip and graphene obtained after stabilization,  $z_{tg}^0$ , could be determined, in principle, by decreasing the distance between tip and sample until the conductance reaches the conductance quantum  $G_0 = 2e^2/h$  [1]. Unfortunately, this does not work for graphene, because the graphene is lifted during the tip approach, even on the hills (reference positions) as indicated from significantly too large decay constants  $\kappa$  extracted from  $I(z)$ -spectra, which have been measured systematically on the graphene surface. The only way to reasonably estimate  $z_{tg}^0$  is to calculate  $\kappa = 23.3 \text{ nm}^{-1}$  with the help of equation 2 (below) and, then, to extrapolate the exponential behaviour of the conductance with respect to the distance by using the stabilization parameters  $U_s = -0.6$  V and  $I_s = 200$  pA:

$$\frac{I_s}{U_s} = \frac{2e^2}{h} \exp \{ -2\kappa(U_s) z_{tg}^0 \}$$

$$\Leftrightarrow z_{tg}^0 = -\frac{1}{2\kappa(U_s)} \ln \left\{ \frac{1}{G_0} \frac{I_s}{U_s} \right\} = 0.56 \text{ nm}. \quad (1)$$

To determine the decay constant  $\kappa(U)$ , we use a planar tunnelling junction with a correction factor  $\xi$  [3]:

$$\kappa(U) = \xi \sqrt{\frac{2m_e}{\hbar^2} \left( \phi_{\text{eff}} - \left| \frac{eU}{2} \right| \right)}. \quad (2)$$

The effective work function  $\phi_{\text{eff}} = (\phi_{\text{gr}} + \phi_t)/2 = 4.89$  eV has been calculated using the known graphene work function of  $\phi_{\text{gr}} = 4.66$  eV [2] and a tip work function of  $\phi_t = 5.11$  eV derived from the measured contact potential as displayed in Fig. 3a of the main text. The correction factor  $\xi = 1.06$  has been determined by fitting  $I(z)$ -curves measured with the same microtip on Au(111) by equation 2 (work function:  $\phi_{\text{Au}} = 5.31$  eV [4]).

**III. CALCULATION OF THE INTERACTION  
POTENTIALS ACTING ON THE  
NANO-MEMBRANE**

In order to describe the observed behaviour of the nano-membrane, the involved interaction potentials are analysed in detail. Besides the electrostatic potential  $\Phi_{\text{el}}$  induced by the tip, the Casimir/van-der-Waals potentials  $\Phi_{\text{vdW}}$  induced by the tip and the  $\text{SiO}_2$ -substrate as well

as the elastic restoring force of the membrane itself  $\Phi_{\text{mem}}$  are considered.

### A. Casimir/van-der-Waals potential induced by the tip

The description of the van-der-Waals and Casimir potential  $\Phi_{\text{vdW}}$  per unit area  $A$  between two materials is given by [5]:

$$\frac{\Phi_{\text{vdW}}}{A}(z_{\text{tg}}) = \frac{\hbar}{4\pi^2} \int_0^\infty k_\perp dk_\perp \int_0^\infty \ln[1 - r_{\text{gr}} r_{\text{w}} e^{-2qz_{\text{tg}}}] d\omega \quad (3)$$

where  $r_{\text{gr}}$  and  $r_{\text{w}}$  denote the frequency dependent reflection coefficients of graphene and tungsten, respectively,  $k_\perp$  is the wave number parallel to the surface,  $z_{\text{tg}}$  is the variable distance between graphene and the tip apex and  $\omega$  is the frequency ( $\hbar$ : Planck's constant). The reflection coefficient of graphene can be calculated by [5]:

$$r_{\text{gr}} = \frac{c^2 q \Omega}{c^2 q \Omega + \omega^2}, \quad (4)$$

with  $\Omega = 6.75 \times 10^5 \text{ m}^{-1}$ ,  $c = 3 \cdot 10^8 \text{ m/s}$  and

$$q = \sqrt{k_\perp^2 + \frac{\omega^2}{c^2}}. \quad (5)$$

To determine the reflection coefficient of the tungsten tip, the frequency dependent dielectric constant  $\varepsilon(\omega)$  has to be used:

$$r_{\text{w}} = \frac{\varepsilon(\omega)q - k}{\varepsilon(\omega)q + k} \quad (6)$$

with

$$k = \sqrt{k_\perp^2 + \varepsilon(\omega) \frac{\omega^2}{c^2}}. \quad (7)$$

The dielectric function can be approximated knowing the plasma frequency of tungsten  $\omega_{\text{p,W}} = 9.74 \times 10^{15} \text{ Hz}$  [7]:

$$\varepsilon(\omega) = 1 + \frac{\omega_{\text{p,W}}^2}{\omega^2}. \quad (8)$$

The total interaction potential  $\Phi_{\text{vdW}}(z)$  is determined by an integration of equation 3 over the circular area of the nano-membrane:

$$\Phi_{\text{vdW}}(z_{\text{tg}}(r' = 0)) = 2\pi \int_0^r \frac{\Phi_{\text{vdW}}}{A}(z_{\text{tg}}(r')) r' dr', \quad (9)$$

where  $z_{\text{tg}}(r')$  denotes the vertical distance between tip and graphene at a lateral distance  $r'$  measured from the centre of the membrane and  $z_{\text{tg}}(r' = 0)$  indicates that we use the tip-graphene distance in the centre of the

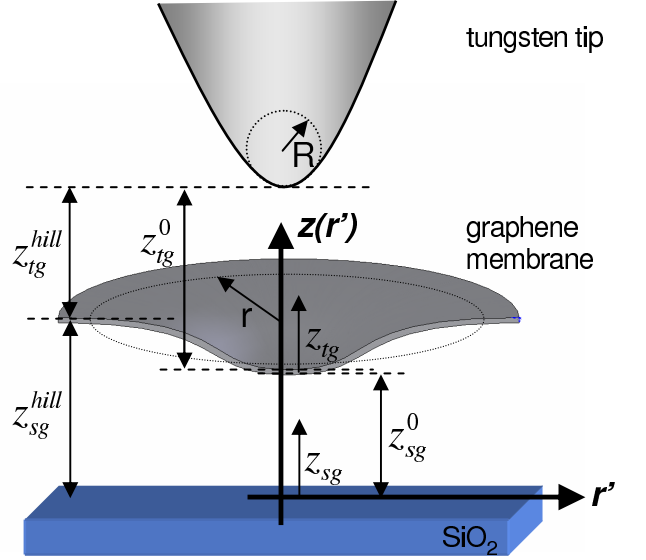


FIG. 2: Definition of distances used in the calculation of the interaction potentials.

membrane as the variable for  $\Phi_{\text{vdW}}$ . Assuming a circular membrane with the measured radius of  $r = 2.58 \text{ nm}$  and a 2D-cosine shaped corrugation (see Fig. 2), as well as a parabolic tip with central radius  $R$ ,  $z_{\text{tg}}(r')$  can be described as:

$$z_{\text{tg}}(r') = \frac{r'^2}{2R} + [z_{\text{tg}}(0) - z_{\text{tg}}^{\text{hill}}] \cos^2\left(\frac{\pi r'}{2r}\right) + z_{\text{tg}}^{\text{hill}}. \quad (10)$$

The vertical distance between tip apex and the hills surrounding the membrane  $z_{\text{tg}}^{\text{hill}}$  is determined by analysing the measured valley depth with respect to the surrounding hills. For the tip radius  $R$  we can only give an upper limit of  $R = 2.3 \text{ nm}$  determined by analysing STM images of atomically resolved valleys, which would not have been resolved by larger tips due to convolution effects. The smallest possible tip radius of  $R = 0.3 \text{ nm}$  is given by a tetraedric alignment of the first four atoms. For the calculation, we use a value of  $R = 0.7 \text{ nm}$ , determined as described below.

### B. Casimir/van-der-Waals potential induced by the SiO2-substrate

The interaction potential between graphene and the amorphous SiO<sub>2</sub>-substrate  $\Phi_{\text{vdW}}(\text{sg})$  is calculated similarly using equation 3–7 and 9, but replacing  $z_{\text{tg}}(r')$  by the distance between graphene and the SiO<sub>2</sub> substrate  $z_{\text{sg}}(r')$  as well as  $r_{\text{w}}$  by the reflection coefficient of SiO<sub>2</sub>  $r_{\text{SiO}_2}$ . In case of an insulating material like SiO<sub>2</sub>,  $\varepsilon(\omega)$  is given by another expression [5]:

$$\varepsilon(\omega) = 1 + \frac{\varepsilon(0) - 1}{1 + \frac{\omega^2}{\omega_e^2}}, \quad (11)$$

where  $\omega_e = 1.05 \times 10^{16} \text{ s}^{-1}$  is the main electronic absorption frequency being within the ultra violet region [8, 9]. For amorphous  $\text{SiO}_2$ , we use the known dielectric constant at zero frequency of  $\varepsilon(0) = 3.9$  [6]. To describe  $z_{\text{sg}}(r')$ , assuming a plane substrate ( $\text{SiO}_2$  shows a corrugation with a preferential distance between hills of 50 nm, thus the assumption of a plane substrate is safe on the range of 5 nm.) and again a 2D-cosine shaped membrane as sketched in Fig. 2, we use

$$z_{\text{sg}}(r') = z_{\text{sg}}^{\text{hill}} - [z_{\text{sg}}^{\text{hill}} - z_{\text{sg}}(0)] \cos^2 \left( \frac{\pi r'}{2r} \right) \quad (12)$$

with  $z_{\text{sg}}^{\text{hill}}$  being the distance between substrate and the borders of the membrane (surrounding hills) and  $z_{\text{sg}}(0)$  being the distance between the substrate and the lowest point of the membrane. The value of  $z_{\text{sg}}(0)$  can vary with the applied voltage  $U$  or with the tip-substrate distance. However, the change of  $z_{\text{sg}}(0)$  with  $U$  or tip-substrate distance can be measured via the tunnelling current. Only the offset of the initial tip-substrate distance,  $z_{\text{sg}}^0$ , without electric field has to be taken as a fit parameter.

### C. Elastic membrane potential

In order to determine the elastic potential  $\Phi_{\text{mem}}$  of the nano-membrane, we assume a cubic force dependence of the deflection  $z_+$  as given by the classical clamped membrane theory according to Komaragiri et al. [11][10]. The nanomembrane gets laterally compressed if lifted until the centre of the membrane is at the same height as the surrounding hills (see Fig. 1c of the main text). If lifted further the membrane gets relaxed again up to a second stable position above the surrounding hills. In order to model this behaviour, we compose the membrane potential  $\Phi_{\text{mem}}$  of two parts  $\Phi^+(z_{\text{sg}}(0))$  and  $\Phi^-(z_{\text{sg}}(0))$  with minima vertically symmetric with respect to the position of largest compression leading to:

$$\begin{aligned} \Phi^+(z_{\text{sg}}) &= -0.265 E^{2\text{D}} \frac{(z_{\text{sg}} - z_{\text{sg}}^{\text{hill}} + \frac{d}{2})^4}{r^2}, \text{ if } z_{\text{sg}} < z_{\text{sg}}^{\text{hill}}, \\ \Phi^-(z_{\text{sg}}) &= -0.265 E^{2\text{D}} \frac{(z_{\text{sg}} - z_{\text{sg}}^{\text{hill}} - \frac{d}{2})^4}{r^2}, \text{ if } z_{\text{sg}} > z_{\text{sg}}^{\text{hill}}, \end{aligned}$$

where  $E^{2\text{D}}$  denotes the two dimensional Young's modulus due to compressing or stretching of the atomic bonds, which has been measured previously to be  $E^{2\text{D}} = 340 \text{ N/m}$  [10]. The distance between the two potential minima  $d$  is the second free parameter of our model, only limited to about twice the valley depth. We found that  $d = 0.12 \text{ nm}$  is able to reproduce the behaviour of the membranes displayed in Fig. 1 and 2 of the main text. This number is lower than the valley depth appearing in the STM images implying that the van-der-Waals force of the  $\text{SiO}_2$  substrate increases the corrugation strength within the graphene flake.

### D. Electrostatic potential induced by the tip

The electrostatic potential  $\Phi_{\text{el}}$  induced by the tip is given by

$$\Phi_{\text{el}} = \frac{1}{2} C_{\text{m}} U_{\text{eff}}^2, \quad (13)$$

with the capacitance  $C_{\text{m}}$  and the effective gap voltage  $U_{\text{eff}}$  to be determined. We approximate the tip-sample system by a capacitor consisting of a sphere with radius  $R$  above a circular plate of radius  $r$  corresponding to tip and membrane, respectively. The capacitance  $C$  for  $r = \infty$  can be calculated analytically resulting in [14]:

$$C = 4\pi\varepsilon\varepsilon_0 R \sinh \left[ R \cosh \left( \frac{z_{\text{tg}} + R}{R} \right) \right] \cdot \sum_{n=1}^{\infty} \sinh^{-1} \left[ n R \cosh \left( \frac{z_{\text{tg}} + R}{R} \right) \right], \quad (14)$$

with the distance between the tip apex and the infinite plate  $z_{\text{tg}} = z_{\text{tg}}(0)$ . The capacitance determined by equation 14 has to be modified because of the finite area of the nano-membrane below the tip. Therefore, we assume a Gaussian shape of the total charge density of the infinite plate with a maximum at  $r' = 0$  to be determined below and calculate the capacitance of the finite membrane by integration only over the circular area of the nano-membrane. We end up with a capacitance  $C_{\text{m}}$  of

$$C_{\text{m}} = C \left[ 1 - \exp \left( -\frac{\pi\varepsilon\varepsilon_0 r^2}{C z_{\text{tg}}} \right) \right]. \quad (15)$$

Because of the finite charge carrier concentration of graphene, the effective voltage  $U_{\text{eff}}$  between the tip and graphene is smaller than the applied bias-voltage  $U$ . The remaining voltage leads to a considerable Fermi level shift within the graphene until the charge carrier density is high enough to screen the electric field. As a consequence, there is a potential drop between the graphene just below the STM tip and the gold electrode connected to the external power supply. Due to the linear dispersion relation of graphene the two dimensional charge carrier density  $n$  can be written as [12]:

$$n = \frac{e^2 (\tilde{U} - U_{\text{eff}})^2}{\pi \hbar^2 v_{\text{F}}^2}, \quad (16)$$

where  $\tilde{U} := U - U_{\text{C}}$  with  $U_{\text{C}}$  being the contact potential determined in Fig. 3a of the main text,  $v_{\text{F}} = 1.1 \times 10^6 \text{ m/s}$  is the Fermi-velocity of graphene and  $e$  is the electron's charge. In equilibrium, the electrons screen the electric field  $E$  and the resulting 2D charge density can be most easily approximated by a plate capacitor leading to:

$$ne = \varepsilon\varepsilon_0 E(U_{\text{eff}}) = \varepsilon\varepsilon_0 \frac{U_{\text{eff}}}{z_{\text{tg}}^+}. \quad (17)$$

Thereby,  $z_{\text{tg}}^+$  denotes the distance between the plate and the centre of mass of the lower half sphere approximating

the tip, which has been chosen to map the model of two parallel plates to the model of a sphere and a plate. With the help of equations 16 and 17, the effective voltage drop between tip and graphene becomes:

$$U_{\text{eff}} = \tilde{U} + \frac{\alpha}{2z_{\text{tg}}^+} - \sqrt{\frac{\alpha^2}{4(z_{\text{tg}}^+)^2} + \frac{\alpha\tilde{U}}{z_{\text{tg}}^+}}, \quad (18)$$

$$\alpha = \frac{\varepsilon\varepsilon_0\pi\hbar^2v_{\text{F}}^2}{e^3}.$$

The value of the dielectric constant for graphene on SiO<sub>2</sub> has been calculated previously using the image potential method and amounts to  $\varepsilon = 2.5$  [13]. The resulting  $n$  calculated straightforwardly by inserting  $U_{\text{eff}}$  into equation 16 has been used self-consistently as the maximum of the Gaussian charge density required to calculate  $C_{\text{m}}$ .

#### IV. EXCITATION OF THE NANO-MEMBRANE BY AC-VOLTAGE

We applied an ac-voltage  $U(t) = U_{\text{dc}} + U_0 \cos(2\pi\nu t)$  with a varying amplitude  $U_0$ , at a dc-offset  $U_{\text{dc}}$  and a frequency of  $\nu = 1.4$  kHz. In addition, we define the voltage  $U^c(t) = U_{\text{dc}} + U_0 \cos(2\pi\nu t) - U_c$  including the contact potential  $U_c$  determined from Fig. 3a of the main text. The time dependent tunnelling currents  $I_0(t)$ , measured at the stable reference position and  $I(t)$  measured above the nano-membrane can be described using the linear graphene density of states as:

$$I_0(t) \propto \frac{U(t)^3}{|U(t)|} \exp\{-2\kappa(U(t))z_{\text{tg}}^0\} \quad (19)$$

and

$$I(t) \propto \frac{U(t)^3}{|U(t)|} \exp\{-2\kappa(U(t)) [z_{\text{tg}}^0 - z_+(U_{\text{eff}}(t))]\}, \quad (20)$$

where  $z_+(U_{\text{eff}})$  denotes the deflection of the nano-membrane with respect to its position in the absence of electric field and  $U_{\text{eff}}(t)$  is the part of the corrected voltage  $U^c(t)$  dropping between membrane and tip. Note, that the expression for  $z_+$  is assumed not to be present on the reference position. The quadratic dependence of the tunnelling current with respect to the bias voltage is derived from the linear dispersion relation of graphene and has been checked by according fits to the measured  $I(U)$ -spectra. In Fig. 3d of the main text, we display the lock-in ratio:

$$r_{\text{LI}} = \frac{\int_t^{t+T} I(t) \cos(2\pi\nu t) dt}{\int_t^{t+T} I_0(t) \cos(2\pi\nu t) dt}, \quad (21)$$

which can be directly used to determine the deflection amplitude  $\Delta z$  numerically as displayed on the right of Fig. 3d of the main text. Accordingly, the upper scale of Fig. 3d of the main text shows the electric field amplitude  $E_0$  given by  $E_0 = U_{\text{eff,max}}/z_{\text{tg,min}}$  with  $z_{\text{tg,min}}$  being the minimal distance between graphene and tip and  $U_{\text{eff,max}}$  being the maximal effective voltage during the oscillation.

Finally, we describe our estimate of the tip radius  $R$ . Therefore, we use the simplified clamped membrane model for the force-deflection curve, consisting of a linear term caused by so-called pretension and a cubic term describing the compression of the atomic bonds given by  $E^{2\text{D}}$  [10]. The equilibrium between the electrostatic force and the elastic membrane force is then given by:

$$\frac{1}{2} \frac{\partial C_{\text{m}}}{\partial z_{\text{tg}}} (U_{\text{eff}}(t))^2 = -\sigma_0^{2\text{D}} \pi z_+ - E^{2\text{D}} 1.06 \frac{z_+^3}{r^2}, \quad (22)$$

where  $\sigma_0^{2\text{D}}$  denotes the two dimensional pretension. After solving towards  $z_+(U_{\text{eff}})$  numerically, we fitted the measured  $r_{\text{LI}}$  taking  $\sigma_0^{2\text{D}}$  and the tip radius  $R$  as the only free parameters. The excellent fit displayed in Fig. 3d of the main text results in a tip radius of  $R = 0.7$  nm and a pretension of  $\sigma_0^{2\text{D}} = 0.62$  N/m.

---

[1] Kröger, J.; Jensen, H.; Berndt, R. *New J. Phys.* **2007**, *9*, 153.  
[2] Shan, B.; Cho, K. *Phys. Rev. Lett.* **2005**, *94*, 236602.  
[3] Ukraintsev, V. A. *Phys. Rev. B* **1996**, *53*, 11176.  
[4] Michaelson, H. B. *J. Appl. Phys.* **1977**, *48*, 4729.  
[5] Bordag, M.; Geyer, B.; Klimchitskaya, G. L.; Mostepanenko, V. M. *Phys. Rev. B* **2006**, *74*, 205431.  
[6] Wilk, G. D.; Wallace, R. M.; Anthony, J. M. *Appl. Phys. Rev.* **2001**, *89*, 5243.  
[7] Ordal, M. A.; Bell, R. J.; Alexander, Jr., R. W.; Long, L. L.; Query, M. R. *Appl. Opt.* **1985**, *24*, 4493.  
[8] Israelachvili, J. *Intermolecular and Surface Forces*, 2nd edition; Academic Press Limited, London, 1992.

[9] Webpage of Heraeus, [http://www.heraeus-quarzglas.de/en/quarzglas/opticalproperties/Optical\\_properties.aspx](http://www.heraeus-quarzglas.de/en/quarzglas/opticalproperties/Optical_properties.aspx)  
[10] Lee, C.; Wei, X.; Kysar, J. W.; Hone, J. *Science* **2008**, *321*, 385.  
[11] Komaragiri, U.; Begley, M. R.; Simmonds, J. G. *J. Appl. Mech.* **2005**, *72*, 203.  
[12] Gusynin, V. P.; Sharapov, S. G. *Phys. Rev. B* **2006**, *73*, 245411.  
[13] Xu, W.; Peeters, F. M.; Lu, T. C. *Phys. Rev. B* **2009**, *79*, 073403.  
[14] Smythe, W. R. *Static and Dynamic Electricity*, 3rd Edition.; (Mc Graw-Hill Inc., 1968).